International Research Journal of Engineering and Technology (IRJET) e-ISSN: 2395-0056
Volume: 11 Issue: 07 | July 2024 www.irjet.net p-ISSN: 2395-0072

Performance Evaluation of a Shielded Metal Arc Welded ENiCrMo-10 Weld cladding on Austenitic Stainless Steel grade 316L

Manish V. Mehta[1,2], Mrunalkumar D. Chaudhari[3*], Jay J. Vora[4*]

[1]*Research Scholar, Gujarat Technological University, Ahmedabad, India,*
[2]*Government Polytechnic, Rajkot, India.*
[3]*Mechanical Engineering Department, L. D. College of Engineering, Ahmedabad, India*
[4]*Mechanical Engineering Department, Pandit Deendayal Energy University, Gandhinagar, India*

Abstract:

Shielded Metal Arc welding with ENiCrMo-10 weld cladding on Grade 316L austenitic stainless steel is examined in this article. This material-process combination is being evaluated for use in petrochemicals, oil, gas, medicines, and chemical processing plants. The weld cladding was assessed through a series of examinations, counting visual inspection, micro hardness, chemical composition study via optical spectroscopy, bend tests and Corrosion resistance testing, while macro and microstructure observations provided additional insights. These observations show numerous remarkable results. A large dilution height of 3.0 mm from the base metal enabled precise control and minimum alloy mixing. Visual inspection and bend tests confirmed cladding weld integrity. The weld cladding's high-quality finish eliminates the need for costly machining and polishing, saving money. The study clarifies main and secondary inter-laminar spacing, improving structural integrity. Weld cladding toughness is also good. The weld cladding's low corrosion resistance must be noted. This research introduces a new material combination and highlights its many benefits for industry stakeholders, notably in the petrochemical and pharmaceutical industries. It improves welding operations and improves industrial applications' efficiency, cost, and structural performance.

Key words: ENiCrMo-10, Shielded Metal Arc Welding(SMAW), Grade 316L,Weld cladding performance

1. Introduction:

The manufacturing industries like chemical, petrochemical, pharmaceutical and oil & gas play a important role in the world economy. They supply variety of materials and products related to chemicals are necessary for numerous region, including energy, manufacturing, and transportation [1]. A major challenge for industries is the corrosive degradation of equipment surfaces. This problem is triggered by wear and corrosive substances that contaminate various parts of manufacturing equipment [2][3]. Degradation can result from erosion, corrosion, or / and friction, either independently or in combination, and is influenced by parameters. To address this issues, a practical preventive measure includes applying protective coatings made from specialized corrosion-resistant materials, considerably reducing degradation of manufacturing equipment [4]–[9].

Responding to rising requirement for surface protecting materials across a variety of applications necessitates inventive resolutions that enhance material life, efficiency, and consistency. So, selecting appropriate protective layers becomes important for ensuring safe operations. Among the effective methods garnering considerable attention are weld cladding techniques, which improve corrosion resistance of parent materials [10], [11].

Weld cladding, a specific technique for enhancing corrosion resistance, plays a important role in safeguarding critical infrastructure and equipment from aggressive environments. This process entails depositing a layer of corrosion-resistant alloy onto a base metal through welding. The primary benefit of this method lies in its capacity to create a protective coating that insulates the underlying material from corrosive agents, including acids, chemicals, and saltwater. By employing weld cladding, industries can significantly extend the operational life of their assets, thereby reducing the frequency of replacements and minimizing maintenance requirements. This technique offers a strategic approach to corrosion prevention, allowing for the targeted application of protective materials to high-risk areas. As a result, it presents a more economical alternative to constructing entire structures from costly corrosion-resistant alloys. The implementation of weld cladding techniques contributes substantially to the overall resilience, longevity, and economic efficiency of industrial equipment and

infrastructure. By mitigating the detrimental effects of corrosion, this method ensures improved performance and reliability in challenging operational environments [12]–[14].

During the weld overlay process, a phenomenon known as welding dilution takes place. This occurs when the heat generated by welding causes the base material to partially melt and intermix with the added filler metal. Welders typically select filler materials for their specific attributes, such as enhanced durability or resistance to corrosive elements. As the intense heat of welding is applied, it not only melts the filler metal but also causes some melting of the base metal at the joint interface. The resulting blend of base and filler metals in the weld pool is what constitutes welding dilution. This interaction between the two metals can significantly influence the properties of the final weld, particularly in the area where the weld meets the base metal.

The level of dilution depends on factors such as the welding process, welding parameters (current, voltage, travel speed), filler metal type, and metallurgical properties of the base metal. Excessive dilution can lead to changes in mechanical properties and corrosion resistance, potentially affecting performance and integrity. Therefore, controlling welding dilution is essential to ensure welds meet the required specifications and maintain desired properties. Skilled welders and proper techniques are employed to manage dilution and achieve consistent, predictable weld characteristics. In critical applications where minimizing dilution is necessary, specialized welding processes and techniques may be used to control the mixing of base metal and filler metal more effectively [4], [15], [16].

Weld cladding is a technique employed to enhance the surface characteristics of a parent material by depositing a superior metal layer through specialized welding methods. To ensure high-quality results in weld cladding, it's crucial to evaluate several geometric aspects of the weld bead. These include its vertical profile, horizontal span, additional buildup, penetration, and the extent to which adjacent beads overlap. These measurements are essential in determining the level of dilution - a concept that quantifies the degree of mixing between the original base metal and the added cladding material during the welding process. In essence, dilution indicates how much the underlying metal integrates with the newly applied layer as they melt and resolidify together. Understanding and controlling dilution is vital for achieving the desired properties in the clad surface, as it directly influences the final composition and performance of the welded area. By carefully managing these parameters, welders can optimize the cladding process to effectively improve the surface qualities of the base metal while maintaining the intended characteristics of the cladding material [17]–[20].

Of the many cladding materials available, ENiCrMo-10 is notable for its high-performance properties as a Ni-Cr-Mo-W alloy. The ENiCrMo-10 alloy, when used for weld cladding, demonstrates exceptional resistance to a broad spectrum of corrosive conditions. Its protective qualities extend to both oxidizing and reducing acidic environments, making it an ideal choice for applications in challenging industrial settings. This alloy finds particular utility in sectors such as chemical processing, petrochemical operations, and pharmaceutical production, where materials are exposed to harsh chemical agents. The primary benefit of applying ENiCrMo-10 through weld cladding lies in its ability to significantly boost the corrosion resistance of the underlying metal. By depositing this alloy onto the surface of a base material, a protective barrier is formed. This layer effectively shields the base metal from the destructive effects of various corrosive substances, including acids, alkaline compounds, and chloride-containing solutions. In environments where the base metal would typically be susceptible to corrosive attack, the ENiCrMo-10 cladding provides a crucial line of defense. This protective function is especially valuable in industrial applications where material integrity is paramount for safety, efficiency, and longevity of equipment and structures [21]–[24].

ENiCrMo-10 weld cladding offers several advantages, though it also presents unique challenges. The distinct metallurgical characteristics of ENiCrMo-10, when compared to common base materials such as austenitic stainless steel or low carbon steel, can lead to complications in creating a robust, flawless weld interface between the substrate and the cladding layer. These differences in material properties often necessitate specialized welding techniques and careful control of welding parameters to ensure a successful cladding application [25]–[30]. These challenges stem from variations in thermal expansion coefficients and melting points [24], [31], [32]. The application of ENiCrMo-10 cladding demands meticulous consideration when determining welding variables, selecting appropriate consumables, and choosing suitable techniques to create a durable and reliable connection between the materials. During the cladding process, ENiCrMo-10 may be susceptible to issues like solidification cracking and hot cracking, especially if suboptimal practices are employed. These problems can arise from factors such as excessive heat input or inadequate surface preparation.

To minimize the occurrence of these complications, it's essential to implement several key strategies. These include utilizing compatible filler materials, implementing precise heat input control measures, ensuring thorough cleaning procedures, Maintaining appropriate interpass temperatures. By adhering to these best practices, welding professionals can significantly enhance the quality and integrity of ENiCrMo-10 cladding applications [33], [34].

Selecting a process for weld cladding entails considering several key factors for a successful and high-quality result. Material compatibility is crucial to avoid issues like cracking and incompatibility between the base and cladding materials. The choice of cladding material should align with desired properties. Determining the required weldoverlay thickness and managing dilution are essential for achieving the desired properties and dimensions. The joint configuration must be assessed to select a welding process suitable for the specific geometry and accessibility. thickness influences the choice of the welding process, with thicker materials favoring submerged arc or flux-cored arc welding, and thinner materials suiting gas metal or tungsten arc welding. Other considerations include required quality, production rate, heat input, accessibility, operator skill, equipment availability, and cost. Common welding processes for weld cladding include GMAW/MIG, GTAW/TIG, SMAW, SAW, FCAW, and PTAW. The final selection should result from a comprehensive assessment of these factors to ensure a durable and successful weld cladding for the intended application.

Choosing the most suitable welding process for weld cladding is a key decision that involves balancing multiple factors to achieve the best results, reduce dilution, and capitalize on the deposition rate. Conventional welding process like SMAW, GTAW, MIG/MAG and SAW are frequently used for tasks such as filling back welding. Among these, SMAW is especially common in smaller and medium-sized industries, though every method has its respective benefits and limitations. Various welding techniques offer different advantages and drawbacks when applied to cladding processes. Traditional methods like Shielded Metal Arc Welding (SMAW) and Gas Tungsten Arc Welding (GTAW) typically result in slower material deposition. On the other hand, Metal Inert Gas/Metal Active Gas (MIG/MAG) procedures, while potentially faster, may introduce issues such as excessive spatter, suboptimal surface finish, and increased dilution rates.

Submerged Arc Welding (SAW) stands out for its ability to deliver high heat input and achieve deeper penetration. However, more advanced technologies have emerged to address specific cladding challenges. These include Cold Metal Transfer (CMT), Hot Wire Technology (HWT), laser cladding, and Plasma Transferred Arc Welding (PTAW). These cutting-edge methods offer several benefits like enhanced control over dilution, accelerated deposition speeds, superior overall cladding quality. It's important to note that while these advanced techniques can yield improved results, they often come with higher equipment costs and require operators with specialized skills and training [35]–[37].

SMAW presents several advantages for weld cladding applications compared to both conventional and advanced welding techniques. Its versatility allows for use in various positions and environments, making it suitable for scenarios where access is limited or the workpiece is difficult to maneuver. Moreover, SMAW equipment is portable and straightforward, offering a cost-effective solution for on-site applications and repairs. Its simplicity also makes it accessible to a wider range of welders, reducing training costs and time [67].

Another significant advantage of SMAW for weld cladding is its ability to work well with dirty or rusty materials, as it is less sensitive to surface contaminants compared to other welding processes. Additionally, SMAW eliminates the need for external shielding gas, as the flux-coated electrode generates its shielding gas when burned. This feature makes SMAW ideal for outdoor or remote applications where gas availability may be limited. While SMAW provides good penetration and fusion for strong welds, When determining the most suitable welding process for a weld cladding application, it is important to assess factors such as the thickness of the materials involved, the welding position, and the available project budget.[65]-[66].

In current times, a noticeable rise in the use of ENiCrMo-10 weld cladding on Grade 316L in numerous industries, particularly in petrochemicals. This rise in popularity can be attributed to the demand for materials capable of withstanding highly corrosive conditions, maintaining structural integrity, and reducing maintenance expenses. This work aims to underwrite to presentinformation and offer appreciated insights into the successful application of ENiCrMo-10 weld cladding on Grade 316L in industries like petrochemicals, oil and gas, pharmaceuticals, and chemical processing.

Cracks in welds between dissimilar materials have been identified in numerous plants, and there are many documented instances of failures in weldments involving different alloys. Hot cracking defects are frequently seen in dissimilar material welding due to thermal contractions from unequal heating and cooling rates during the welding process. As a result, research

has been directed at finding ways to evaluate and repair structural integrity. To control crack growth and enhance weld thickness and corrosion resistance, shielded metal arc welding (SMAW) is commonly used for cladding. Manual SMAW cladding is especially suitable for repair and maintenance of critical areas due to its versatility[64]-[66].

To achieve this objective, the research paper focuses on investigating the Gas Tungsten Arc welding process for applying ENiCrMo-10 weld cladding on Grade 316L. A range of testing methods will be applied in this study, including visual test (VT) and micro hardness tests, side bend testing, and chemical composition analysis. The Potentiodynamic Polarization Technique will be used for corrosion resistance evaluation, and the research will also include observations of macro and microstructures and an analysis of dilution.

The outcomes of this research hold significant importance for the various critical industrial applications, as they provide valuable insights into effectively applying ENiCrMo-10 weld cladding on Grade 316L. The findings can lead to improved material performance, cost-effectiveness, and reliability in critical industrial environments. Moreover, the study aligns with the growing trend of utilizing ENiCrMo-10 weld cladding on Grade 316L, making it a precious source for researchers and industry professionals in the area of materials engineering.

2. Experimental Process

In this investigation, the SMAW method used to experimentally deposit ENiCrMo-10 flux-coated solid filler wire onto Austenitic stainless steel Grade 316L. The study aimed to evaluate the fitness of this welding methods and material grouping for application in present industrial contexts.

2.1 Material

ENiCrMo-10 alloy was applied to Grade 316L steel using the SMAW methods. Table 1 displays the nominal chemical compositions of both Hastelloy C-22 and Grade 316L steel.

Table 1. Nominal Chemical Composition (Wt. %) for Grade 316L Austenitic Stainless Steel and ENiCrMo-10 Alloy in the Present Work

Elements	C	Si	Mn	P	S	Cr	Mo	Ni
Base Metal Grade 316L	0.023	0.3	1.26	0.043	0.004	16.25	2.03	10.05
ENiCrMo-10	0.01	0.2	0.1	0.003	0.004	20.7	14.5	Bal.
Element	Fe	N	Co	W				
Base Metal Grade 316L	Bal.	0.038	-	-				
ENiCrMo-10	5.1	---	0.06	2.8				

The material under investigation in this study was Grade 316L, with a thickness of 10mm. Its nominal chemical composition is detailed in Table 1. Plates of Grade 316L were precisely cut and machined to dimensions of 500mm x 300mm x 10mm.

2.2 Method

In the current research endeavor, The SMAW process is employed to apply Hastelloy Mo-10 alloy weld cladding onto Grade 316L, to capitalize on the manifold benefits this process offers. Initially, a total of 5 bead-on-plate trials were conducted to meticulously select and screen welding parameters suitable for this research. The choice of parameters for these trials was guided by the recommendations provided by the consumable manufacturer, insights gleaned from literature surveys, and the wealth of industrial experience with this process [25], [37], [38], [47], [52]. This research project involved conducting a series of individual welding passes on a bead-on-plate setup. The experiment was repeated five times to ensure reliability of results. The primary objectives were to examine the operational aspects of the welding process and to investigate how variations in

welding energy influenced specific geometric features of the weld bead. The key characteristics under scrutiny included the height of the weld reinforcement, the ratio between reinforcement height and bead width, the extent of dilution occurring during the welding process. By focusing on these parameters, the study aimed to provide insights into the relationship between welding energy input and the resulting weld bead geometry.

The optimal operating parameters were established through a combination of dilution analysis and visual inspections of the bead-on-plate specimens. These parameters were subsequently applied to welding coupons, as illustrated in Figure 1.

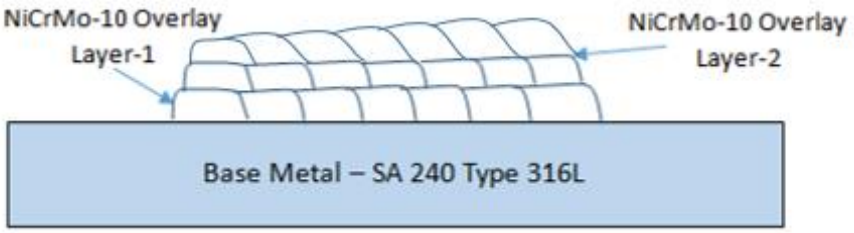

Figure1:weld cladding of Hastelloy MO-10

Proper melting and strong adhesion, particularly at the vertex, must be ensured by the process parameters, while preventing excessive dilution and avoiding defects due to rapid cooling. Shielded Metal Arc Welding process was used to apply three layers of ENiCrMo-10 weld cladding to the Grade 316L base plate. Each layer included ten welding beads. Table 2 outlines the pertinent process parameters, including welding current, voltage, travel speed, and other relevant factors.

Table 2. Welding parameters

Parameter	Layer -1	Layer -2	Layer -3
Current (Amp.)	95-110	100-112	100-118
Voltage Max. (V)	18-22	18-22	18-24
Travel Speed Average (mm/Min)	250-300	280-300	300-320
Filler Wire Dia. (mm)	3.15	3.15	3.15
Polarity	DCEP	DCEP	DCEP
Welding position	1G (Flat)	1G (Flat)	1G (Flat)
Heat Input (Kj/mm)	0.58	0.53	0.57
No. of bead / Layer	10	10	10

In preparation for the welding process, the substrate's top surface underwent thorough cleaning with ethyl alcohol to remove any contaminants. The team then employed the Shielded Metal Arc Welding (SMAW) technique to apply three layers of Hastelloy MO-10 alloy weld cladding, resulting in an initial thickness of approximately 7 mm for both the substrate and the deposited layer. Post-welding visual inspection revealed uniformly smooth welds without noticeable defects. To further ensure quality, non-destructive testing was conducted, focusing on identifying potential issues such as cracks, discontinuities, and interface defects in the cladding. This comprehensive approach aimed to verify the integrity and soundness of the weld cladding application, ensuring that the final product met the required standards for performance and reliability.

2.2.1 Bend test

Bend testing serves as a crucial evaluation method for Hastelloy weld claddings, offering key insights into their performance characteristics. This technique subjects the cladding to specific bending stresses, allowing for the assessment of

its flexibility, durability, and overall structural soundness. By doing so, it helps identify potential defects or weak points that might not be apparent through other inspection methods. The process also verifies compliance with industry-specific standards, ensuring that the cladding meets the stringent requirements of its intended applications. For manufacturers and end-users alike, bend testing provides a reliable means to gauge the cladding's ability to withstand operational demands, thereby confirming its suitability for use in challenging industrial environments. This comprehensive approach to quality assurance contributes significantly to the confidence in the long-term performance and reliability of Hastelloy weld claddings [20], [27], [53]. The reliability assessment of the welded cladding, particularly focusing on the cladded layers, involved subjecting two specimens to side edge bend tests in accordance with BS EN ISO 5173:2010/A1:2011 standards. This comprehensive evaluation targeted ENiCrMo-10 Hastelloy MO-10 weld cladding applied to Grade 316L material using the SMAW process. The testing regimen aimed to thoroughly examine the cladding's weldability, ductility, structural integrity, and overall quality. Utilizing a Digital Universal Testing Machine (model UTE-60) manufactured by FIE, the bend tests were carried out meticulously. The results of these tests successfully met the acceptance criteria outlined in BS EN ISO 15614-7:2019, providing strong evidence of the cladding's performance capabilities and its adherence to industry standards. This rigorous testing approach ensures that the welded cladding meets the stringent requirements necessary for its intended applications, offering confidence in its reliability and durability under various operational conditions.

2.2.2 Hardness test

Evaluating the mechanical properties and integrity of Hastelloy MO-10 weld claddings relies heavily on hardness testing. This method offers crucial insights into the material's quality, the integrity of the weld, the heat-affected zone's characteristics, adherence to acceptance standards, and quality control procedures.[37], [54], [55].

To verify the mechanical properties of the weld cladding and ensure its suitability for the intended application, a series of hardness tests were performed. The evaluation process involved examining transverse cross-sections of the welded specimens using a Leco Vickers hardness tester (Model: M-400A). Hardness measurements were taken at multiple strategic points, encompassing the weld area, heat-affected zone, and base metal, employing a 1000 gf load. This comprehensive testing approach, conducted in accordance with EN ISO 9015-1:2011 standards, provided a detailed hardness profile across the various regions of the welded specimen. The specific locations of the hardness testing points were clearly illustrated in the accompanying Figure 2, offering a visual representation of the test methodology. By systematically assessing the hardness distribution, this analysis helps to confirm the overall integrity and performance characteristics of the weld cladding, ensuring it meets the required mechanical specifications for its intended use.

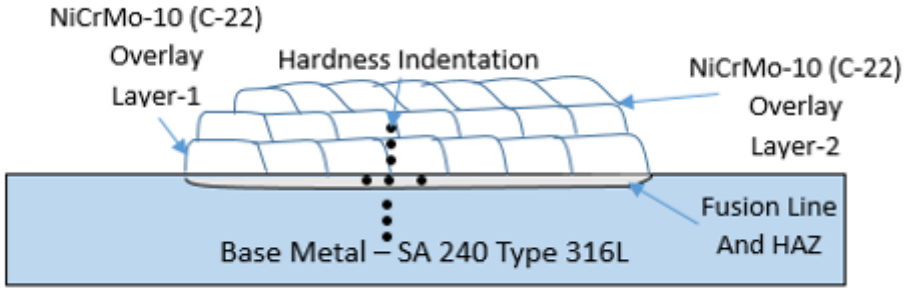

Figure2.LocationHardness Indentation

2.2.3 Macro and Microstructure Examination

Conducting a thorough evaluation of Hastelloy MO-10 overlays on Grade 316L stainless steel is crucial for determining weld integrity, detecting flaws, and verifying adequate bonding and penetration depth. This analysis is vital to ensure the cladding meets quality standards and performs as intended in corrosive environments [2], [56]. Conducting a detailed inspection is crucial for evaluating the durability and dependability of the overlay welding. This process plays a key role in improving the overall functionality and lifespan of the welded connection.

The macroscopic analysis involved cutting AISI 316L plates with Hastelloy MO-10 cladding, originally 500x300x10 mm, into smaller 10x300x10 mm samples. These were then subjected to a progressive polishing regimen using silicon carbide abrasive papers of increasing fineness (120, 320, 400, and 600 grit), followed by alumina powder polishing. The specimens were subsequently etched with Kalling's reagent. Examination was carried out using a Metlab Stereo Zoom Microscope at 10X magnification.

Microstructural investigation is essential for evaluating key material properties including tensile strength, hardness, malleability, and resistance to corrosion. It reveals crucial information about grain morphology, phase composition, and the presence of any structural imperfections or precipitates that could affect material behavior. This research also delves into the characteristics of grain boundaries, phase distribution patterns, and the role of alloying elements in enhancing corrosion resistance [5], [8], [38], [55].

To conduct microstructural examination of the Hastelloy overlay welds, specimens measuring 10x300x10 mm were further reduced to 20x10x10 mm using a precision micro wire electrical discharge machining (EDM) process. These smaller samples underwent a meticulous surface preparation sequence. This involved progressive grinding with silicon carbide abrasives of increasing fineness, starting at 120 grit and proceeding through 320, 400, 600, 800, 1000, and 1200 grit. The final polishing stages utilized alumina powder and diamond paste to achieve a mirror-like 1 µm surface finish. A Metlab optical microscope was then employed to investigate the microstructural features across the weld overlay, heat-affected zone (HAZ), and substrate material.

The spacing of primary and secondary dendrites in weld claddings is a key microstructural parameter that affects mechanical strength and corrosion resistance. Irregularities or variations in dendrite spacing may suggest issues such as hot cracking, lack of fusion, or defects due to the solidification process, potentially compromising weld quality. This research analyzed primary and secondary dendrite spacings in Hastelloy MO-10 weld claddings on Grade 316L using the Shielded Metal Arc Welding (SMAW) technique, with detailed observations and measurements made using the Olympus DSX-1000 digital microscope.

2.2.4 Corrosion resistance using Potentiodynamic Polarization technique

The Potentiodynamic Polarization method is employed to evaluate the corrosion resistance of various materials, including Hastelloy MO-10. This electrochemical technique provides crucial data on the corrosion behavior of Hastelloy MO-10, which is important for selecting appropriate materials, optimizing conditions, and enhancing performance and durability in aggressive environments. In this study, clad samples with dimensions of 10mm by 10mm were tested for corrosion resistance in a ferric sulfate and sulfuric acid solution, with the Gramy Interface 1010E potentiostat used for the corrosion analysis.

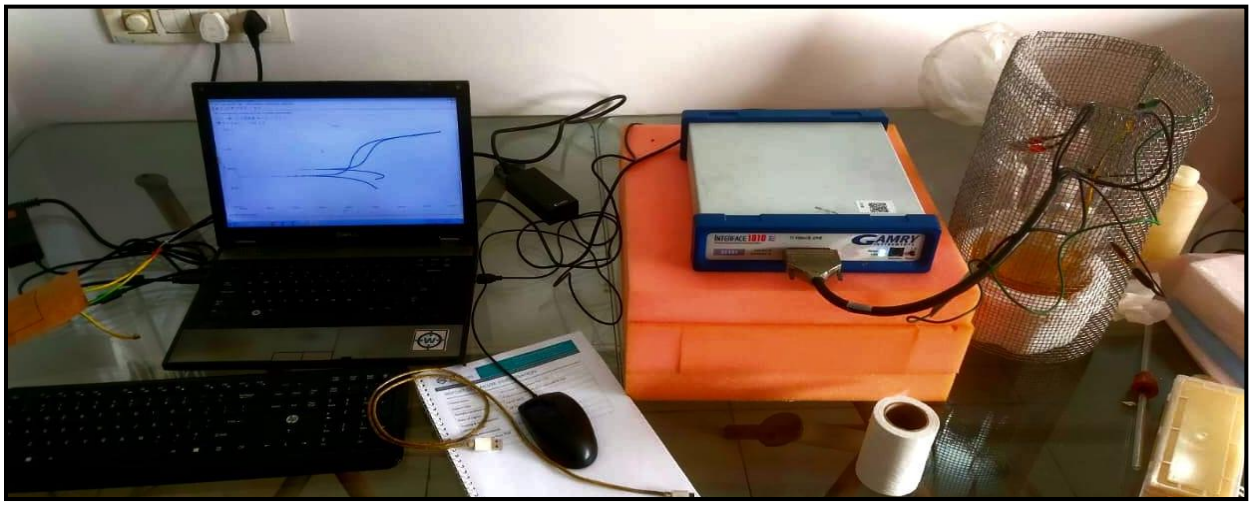

Fig.2 Experimental Setup of Potentiodynamic Polarization Technique

2.2.5 Chemical Composition Test

Optical spectroscopy is a vital method for analysing the chemical composition of weld cladding samples, which ensures material quality, consistency, and performance in corrosive environments. This analysis helps verify that the cladding provides reliable and long-lasting protection. In this study, chemical composition was studied by an optical spectroscopy device by Hitachi Foundry Master Pro-2, with samples analysed at different thicknesses as demonstrated in Figure 3. The sample removal process adhered to ASME Section 9 Figure QW-462.5(a), and testing was performed according to ASTM E-3047-16 standards.

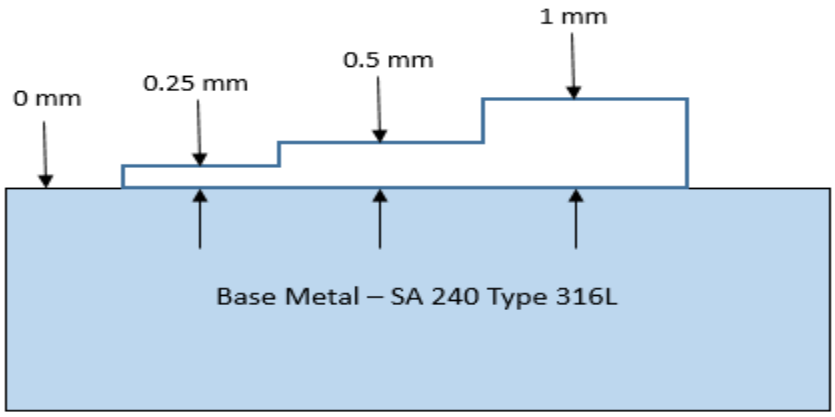

Figure 3. Weldcladding Machining for Chemical composition study

3. Results and discussion

3.1 Visual Analysis

Upon visual inspection, both the Austenitic Stainless Steel 316L and Hastelloy Weld cladding exhibited impeccably clean surfaces without any discernible welding imperfections. Notably, there were no indications of spatter, undercutting, porosity, lack of fusion, inclusions, or cracks, aligning with the expected outcomes described in the literature and highlighting Hastelloy's commendable weldability [6], [50], [51]. However, there remains a gap in our understanding regarding the reaction of the ENiCrMo-10 weld cladding to fusion and solidification rates inherent in welding processes, particularly when utilizing the Shielded Metal Arc Welding (SMAW) technique. The upper surface of the ENiCrMo-10 weld cladding, applied onto an SS-316L substrate, is depicted. Notably, the Hastelloy weld cladding displays a flawless surface, devoid of any welding imperfections such as spatter, undercutting, porosity, lack of fusion, inclusions, cracks, or other irregularities.

The welding conditions utilized in this investigation have directly influenced the quality of the claddings. The exceptional quality of the cladding material is intricately linked to the precise selection of welding parameters. Critical elements contributing to this quality encompass proficient welding techniques and ensuring an appropriate lateral overlap of each pass. The surface quality of the cladding is deemed satisfactory due to the inherent geometric uniformity across the coated area, the absence of flaws, and the minimal occurrence of splattering, all indicative of a high standard of craftsmanship.

3.2 Macro Structure Examination

The material underwent a macroscopic examination at 10x magnification, as shown in Figure 4. The sample was macro-etched, visually inspected, and subsequently magnified 10 times under a microscope. This process facilitated the examination of the cross-section of the Hastelloy MO-10 weld cladding on austenitic stainless steel 316L.

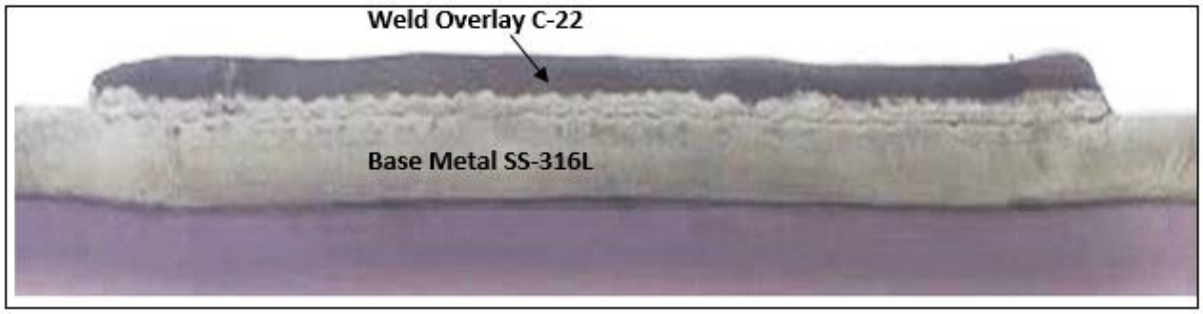

Figure4. Hastelloy Weld cladding Cross Section Visual Test

Figure 4 presents a cross-sectional view of the weld cladding and the base metal, demonstrating the absence of welding defects. Additionally, the cross-section highlights minimal penetration of the Hastelloy weld cladding into the base metal, a characteristic often associated with the heat input inherent in the SMAW process [37], [40], [49], [59]. The line depicted in the figure delineates the extent of penetration of the weld cladding metal into the base metal.

3.3 Bend Test Analysis

To assess the reliability and weldability of the procedure, we implemented the optimal parameters derived from previous tests on actual samples of weld cladding. In this study aimed at enhancing production cost efficiency, we employed AISI 316 L SS cladding with two layers of Hastelloy MO-10. Our primary goal was to ascertain whether these parameters would yield welds devoid of typical issues such as holes or cracks frequently encountered in weld cladding. Additionally, we scrutinized for any indications of excessive hardening in the cladding layer or insufficient integration between the cladding layer and the AISI 316 L SS substrate.

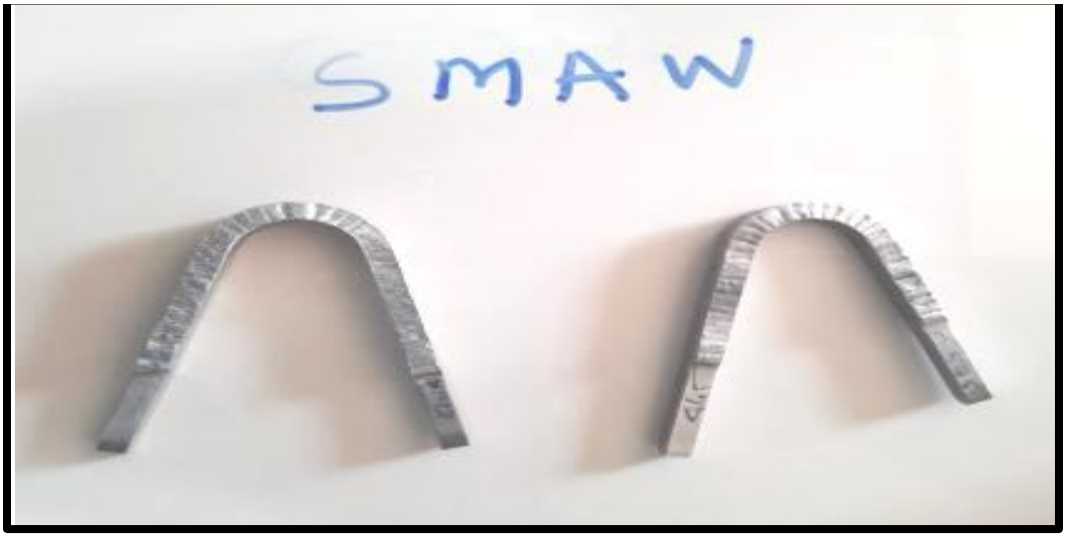

Figure5. Hastelloy Weld cladding bend test by LBW

According to AWS guidelines, defects larger than 3 mm, such as holes or cracks, should not be present, regardless of orientation, even if the specimen prepared for bending is on the surface or side. Figure 5 illustrates that no cracks appeared anywhere on the specimen during the two instances of the side bend test using universal testing equipment. These results offer evidence that the parameters used for this research in weld conditions were without a doubt optimal.

3.4. Hardness testing

The Vickers hardness outline of the thick coating's cross-section is outlined in Table 3. The findings can be summarized as follows:

The base metal's hardness, notably lower compared to the welding overlay and heat-affected zone (HAZ), remains relatively stable at approximately 206Hv. The weld cladding exhibits an average hardness of about 239Hv. This increase in hardness can be attributed to the evolution of microstructure during the welding process. It is widely acknowledged that microstructure and Vickers hardness are closely linked, with a finer microstructure typically resulting in higher hardness, assuming the phase composition remains constant. Both the HAZ hardness and the interface demonstrate a higher hardness level, approximately 256Hv. There is a notable increase in hardness observed from the HAZ to the coating interface.

Table – 3 Vicker Hardness along the Hastelloy MO-10 weld cladding on SS-316L

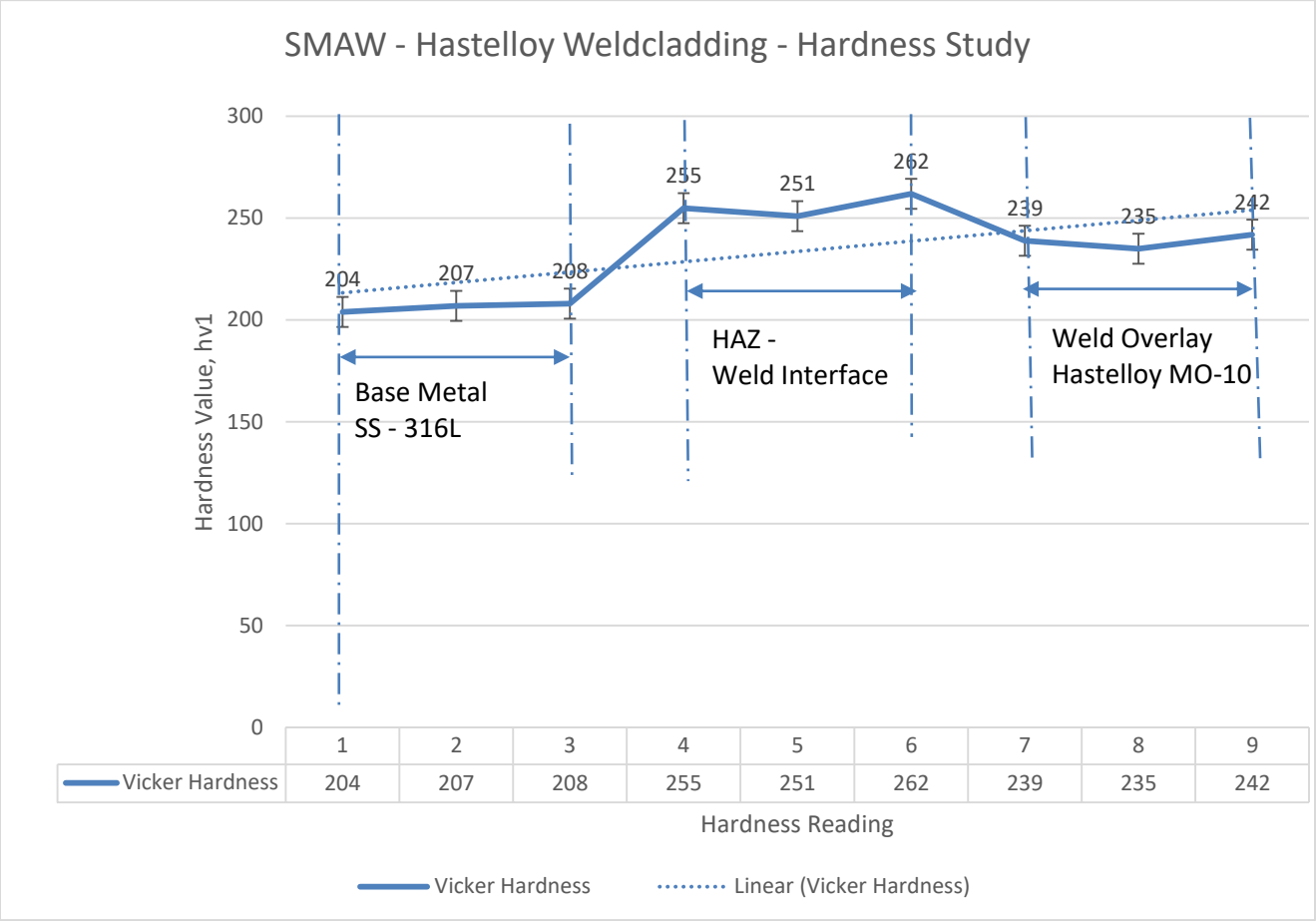

The Vickers hardness profile of the Hastelloy MO-10 weld cladding on the Grade 316L stainless steel cross-section reveals that the parent metal maintains a constant hardness level at approximately 206Hv. This value is notably lower compared to the hardness levels of the coating and the heat-affected zone (HAZ), which measure 239HV and 256HV, respectively. The changes observed in the solidified morphology of the cladding layers can be attributed to the dilution effect, which directly influences the hardness of the cladding weld.

The heat input during the welding process emerges as a significant parameter influencing morphological changes in the weld cladding, particularly when the same combination of weld cladding and substrate is employed. Consequently, it can

be inferred that the heat input directly impacts hardness, dilution, and the width of the heat-affected zone. Our ongoing research, along with findings from relevant literature, supports the assertion that the SMAW process involves significant heat input.

The microstructure morphology, influenced by heat input, plays a crucial role in determining the metal's hardness. Moreover, studies indicate that a notable reduction in the size of primary dendrites generally leads to an increase in Vickers hardness. Presently, the average hardness of the weld cladding slightly surpasses the maximum hardness (100 HRB, 248Hv) stipulated in the ASME code. This elevated hardness can be attributed to laminar separation induced by the rapid cooling rate and low-intensity input.

In this specific case, the SMAW technique showcases a remarkably low heat input, resulting in a finely developed HAZ and weld interface. Consequently, the hardness values at the HAZ and weld cladding are nearly identical.

3.5. Chemical Composition

Industries involved in manufacturing heat exchangers and pressure vessels commonly employ multilayer coatings to mitigate dilution effects and maintain the integrity of chemical composition in the weld metal. This optimization practice is considered crucial for all material combinations, encompassing both the substrate and the deposited alloy. It is universally acknowledged that both the base metal and the weld metal significantly influence the extent of material dilution.

As discussed earlier, the cladding procedure in this scenario induces dilution between the AISI 316L SS substrate and the Hastelloy-22 cladding layers. Table 4 presents the outcomes of optical spectrometry analysis, a widely utilized method in the manufacturing sector for assessing chemical composition. This table utilizes a graphical representation to illustrate the gradients in chemical composition within the AISI 316L SS substrate and the two ENiCrMo-10 cladding layers, emphasizing the dispersion of key alloying elements such as Ni, Cr, Mo, W, and Fe. The graph depicts variations in elemental presence from the interface of the weld layer to the upper surface.

It is noteworthy that the most pronounced changes in composition gradient occur at the interface linking the substrate and the initial cladding layer. Within the region where the weld cladding is present, the chemistry of ENiCrMo-10 is achieved at a point starting from a distance of 3 mm and onward. Beyond this threshold, the composition profiles within the weld cladding regions exhibit marked similarity. Regarding Table 4, the horizontal axis represents the distance in millimeters from the interface, with the chemical composition of ENiCrMo-10 depicted at the terminal point of the axis. The vertical axis denotes the percentage of chemical composition. The graphical representation highlights that the chemical composition of MO-10 closely approximates the desired composition starting from a height of 2.5 mm from the interface. However, the Fe content does not meet the requirements. Yet, from a height of 3 mm onwards, the chemical composition aligns with the MO-10 chemistry. This indicates the possibility of attaining the MO-10 chemical composition at a depth of 2.5 mm with precise parameter selection.

Table – 4 Chemical Composition Gradient Within SS-316L substrate and ENiCrMo-10 weld cladding

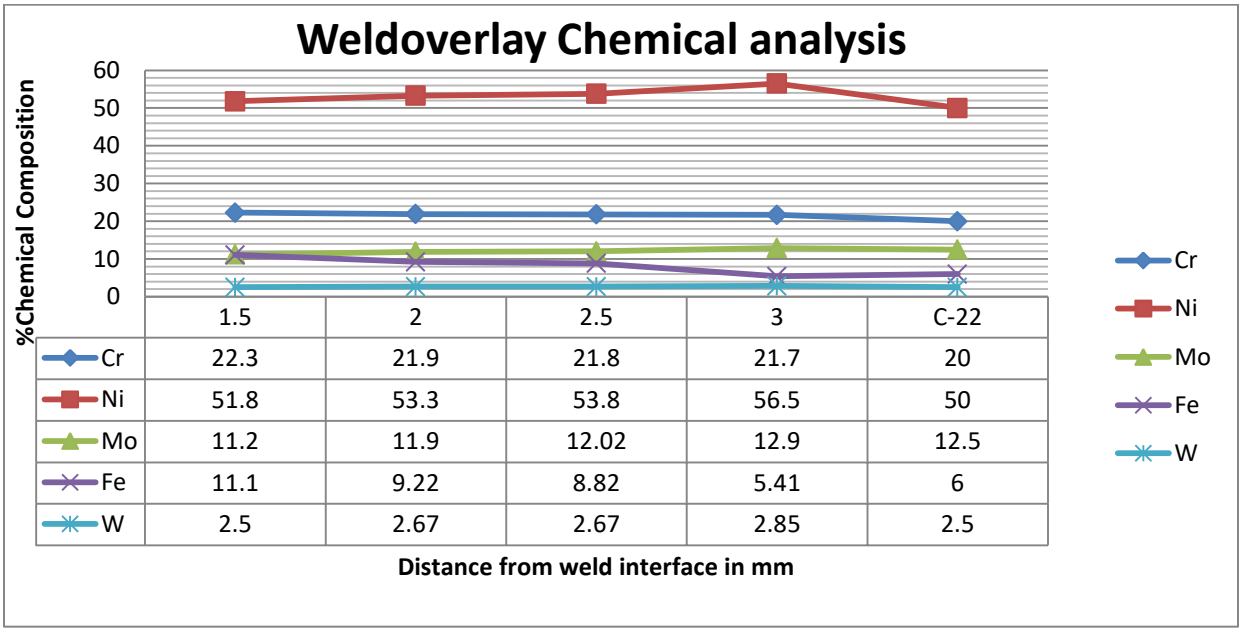

	1.5	2	2.5	3	C-22
Cr	22.3	21.9	21.8	21.7	20
Ni	51.8	53.3	53.8	56.5	50
Mo	11.2	11.9	12.02	12.9	12.5
Fe	11.1	9.22	8.82	5.41	6
W	2.5	2.67	2.67	2.85	2.5

3.6. Microstructure analysis

The microstructures of both the 316L SS substrate and the three ENiCrMo-10 cladding layers underwent a thorough examination. High-magnification optical microscope images were utilized to create a composite image of the Hastelloy weld cladding on the 316L SS sample, as depicted in Figure 6. These micrographs bear a close resemblance to macro images. The stitched image exposes the presence of porosity, lack of fusion, and a defect-free weld cladding of Hastelloy MO-10 on the 316L SS substrate achieved through SMAW. Furthermore, the cross-sectional micrographs vividly illustrate that the microstructure of the SS 316L substrate remains unaltered after the cladding.

The Shielded Metal Arc welding process, characterized by low heat input, yielded no observable heat-affected zone, as confirmed by cross-sectional optical microstructure analysis.

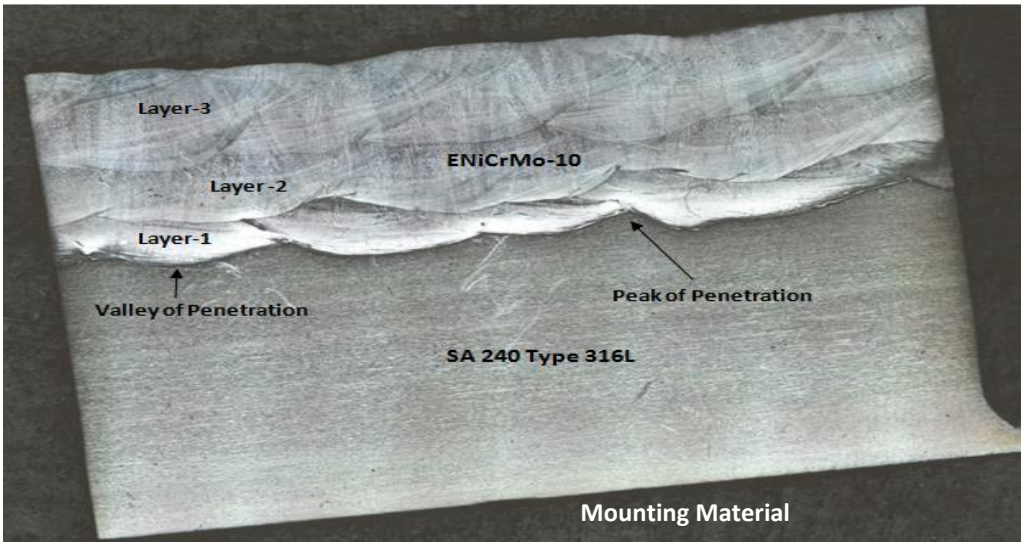

Figure 6. Stitching image of HastelloyWeldcladding of MO-10 on SS-316L

Figure 7 illustrates the morphology and microstructure of the weld cladding regions. Figures 7(a) and (b) provide a view of the morphology at 100X and 200X magnifications, respectively, of the deposited weld cladding. Figures 7(c) and (d) depict the 100X and 200X magnification morphology of the heat-affected zone (HAZ) microstructure. Finally, Figures 7(e) and (f) display the microstructure of the base metal.

In Figures 7(c) and (d), it is evident that a smooth fusion line or distinct fusion bonding interface has been achieved between the Hastelloy MO-10 weld cladding and the SS 316L base metal. Additionally, owing to the low heat input of the process, a small and insignificant HAZ is formed. Figures 7(a) to (f) exhibit microstructures devoid of porosities, cracks, and other defects.

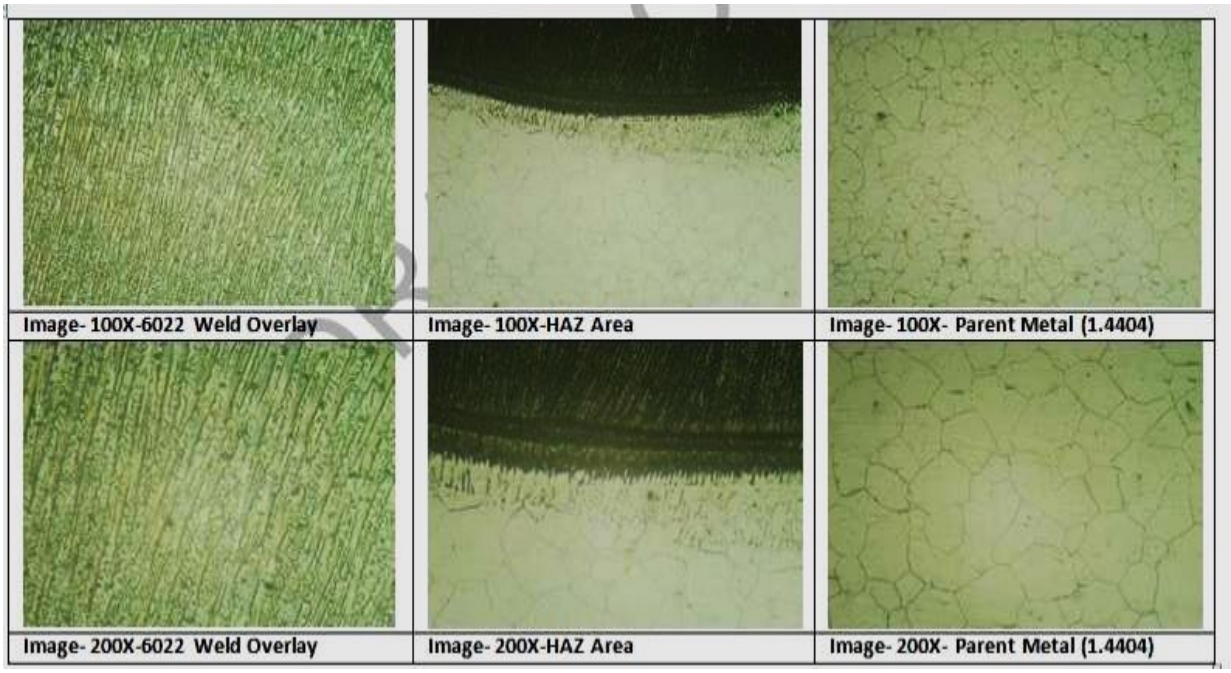

Figure.7 – Microstructure analysis of Hastelloy MO-10 weld cladding on SS-316L

The formation of microstructure is primarily influenced by various factors, including the alloy's composition, the temperature gradient (G), the energy at the interface, and the solidification rate (R). The critical factor determining the morphology of the microstructure during solidification is the ratio between G and R. Figures 7(a) and (b) offer a clear depiction of a fine columnar interdendritic microstructure within the weld cladding. In contrast, Figures 7(c) and (d) reveal a relatively compact heat-affected zone (HAZ) located at the weld interface between the base metal and the weld metal. The presence of this confined and inconspicuous HAZ, alongside the development of the columnar interdendritic microstructure, can be attributed to the utilization of a Shielded Metal Arc Welding (SMAW) process characterized by controlled heat input in these experiments. Furthermore, the micrograph representing the base metal distinctly showcases the emergence of an equiaxed austenite structure, highlighting a unique microstructural characteristic.

Table -5 Primary dendritic arm spacing of Hastelloy weld cladding of MO-10 on SS-316L by SMAW process

Primary Dendritic Arm Spacing (µm)

	Minimum	*Maximum*	*Average*	*Total Reading*
Value (µm)	*3.339*	*3.826*	*3.576*	*4*

Table -6. Secondary dendritic arm spacing of Hastelloy weld cladding of MO-10 on SS-316L by SMAW process

Secondary Dendritic Arm Spacing (µm)				
	Minimum	*Maximum*	*Average*	*Total Reading*
Value (µm)	*3.251*	*4.083*	*3.601*	*4*

Tables 5 and 6 present the average and individual values, respectively, of the primary and secondary interdendritic arm spacing, measured in micrometers (µm). The difference in measurement values between primary and secondary dendrite arm spacing is observed. The results indicate that the average value of secondary arm spacing is comparatively smaller.

Figure 8 displays the primary dendritic arm spacing of the Hastelloy weld cladding, with a total of 4 readings taken. The maximum value of primary dendritic arm spacing is 3.826 µm, while the minimum value is 3.339 µm. The average of these readings is 3.576 µm. In the Arc deposition process, the moderate cooling rate of the melt pool, and consequently the rapid solidification velocity, result in a spacing of primary dendritic arms and secondary dendritic arm spacing [33], [37], [38], [46], [48], [49], [60]–[63], as shown in Figure 8.

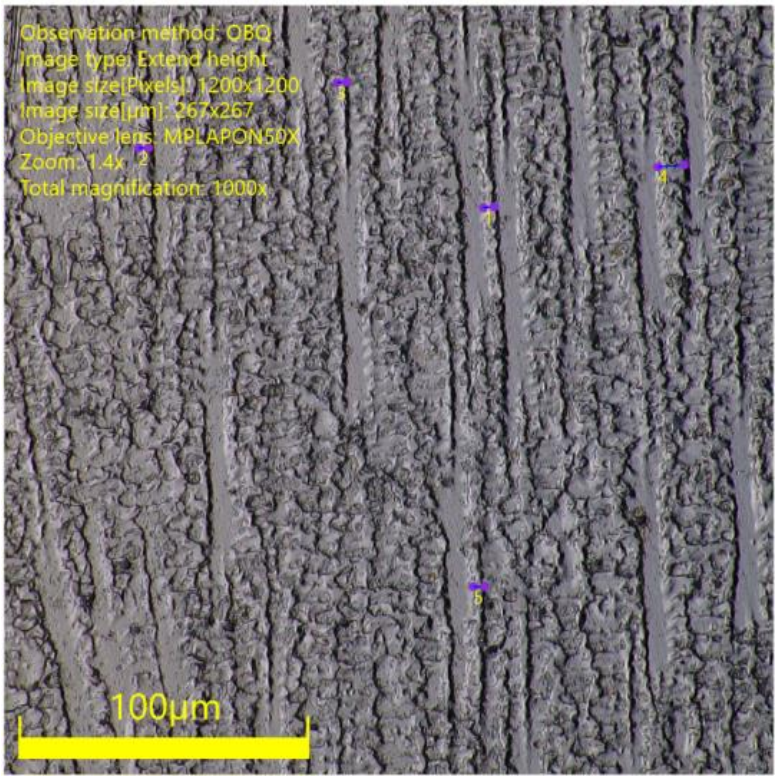

Figure 8. Primary Dendritic Arm Spacing of Hastelloy Weld Cladding by SMAW at 1000X

Furthermore, the solidification velocity of the melt pool facilitates the proper growth of secondary dendrites, as depicted in Figure 9. The average value of secondary dendritic arm spacing obtained through the SMAW Process is 3.601 µm. Dendrite spacings are generally correlated with mechanical strength, hardness, toughness, and corrosion resistance due to factors such as the distribution of alloying elements, segregation, and susceptibility to intergranular corrosion. Both primary and secondary dendrite spacings can significantly influence the integrity of the weld cladding, as supported by references [33], [37], [38], [46], [48], [49], [60]–[63].

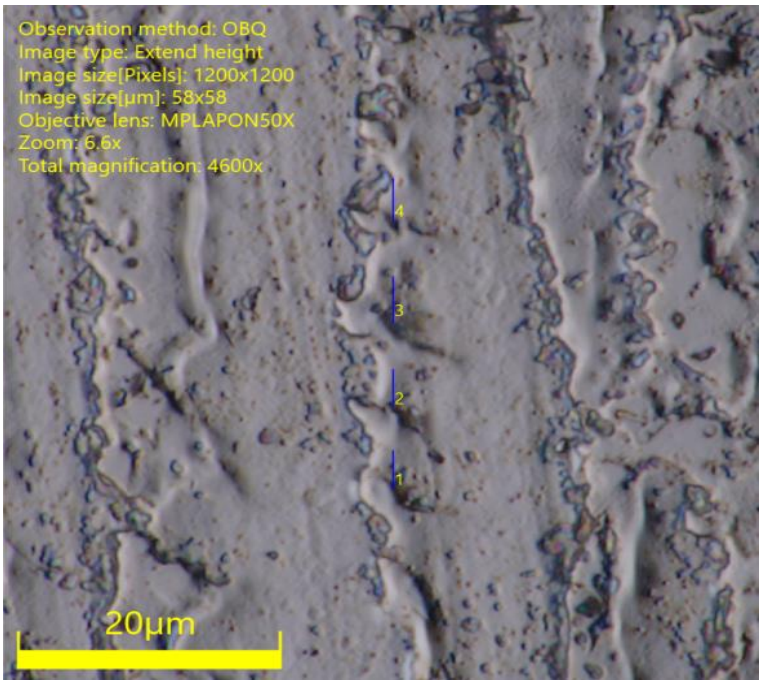

Figure 9. Secondary Dendritic Arm Spacing of Hastelloy Weld Cladding by SMAW at 4600X

3.7. Corrosion Potential Test

Cyclic Potentiodynamic Polarization tests were conducted on the Hastelloy MO-10 weld cladding in a Ferric Sulfate – 50% sulfuric acid solution, following ASTM G-28, Method-A guidelines. Figures 10, 11, and 12 illustrate the potential polarization behavior of the SMAW cladding of the Hastelloy MO-10 weld cladding on SS 316L. These figures also display the potentiodynamic polarization curves obtained from various locations within the Hastelloy MO-10 weld cladding.

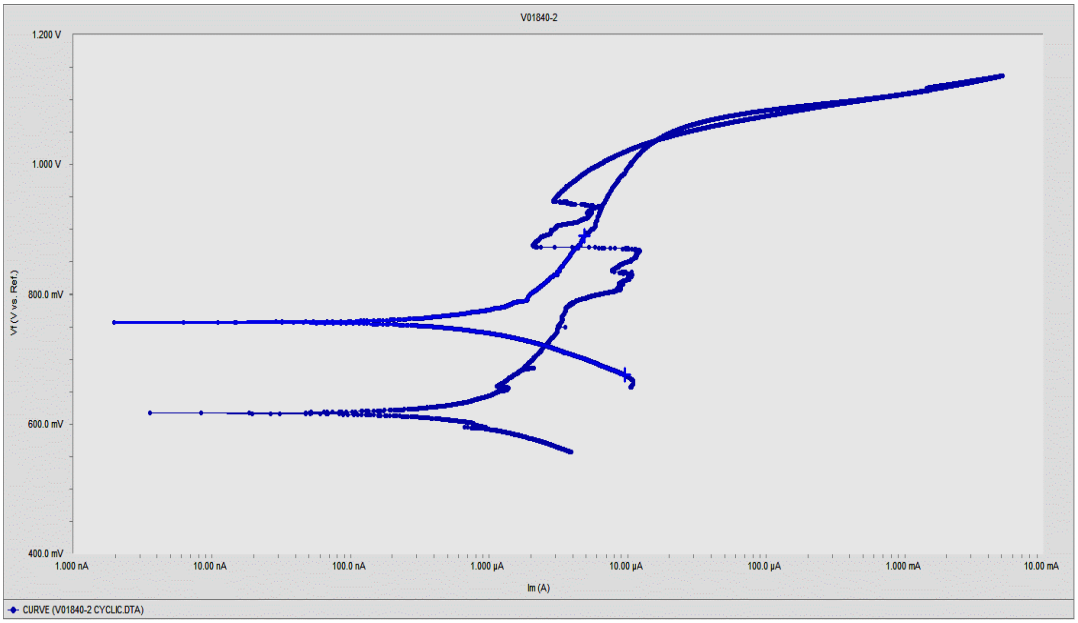

Fig10. Polarization Curve of Hastelloy MO-10 weld cladding, Location.1

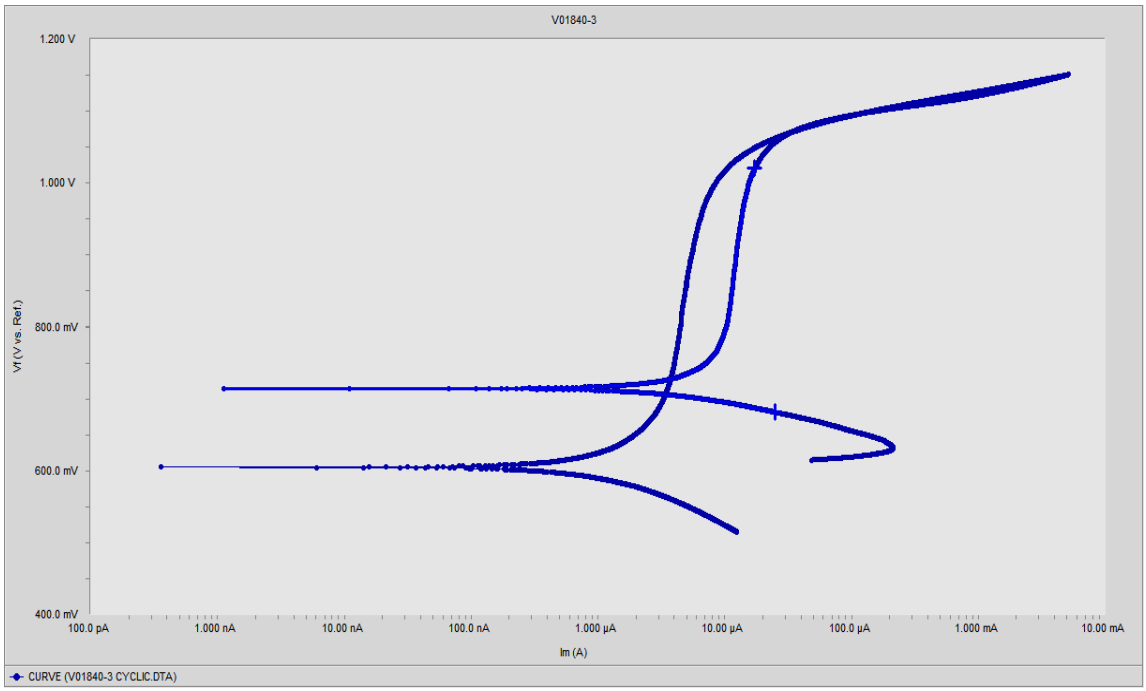

Fig.11 Polarization Curve of Hastelloy MO-10 weld cladding, Location.2

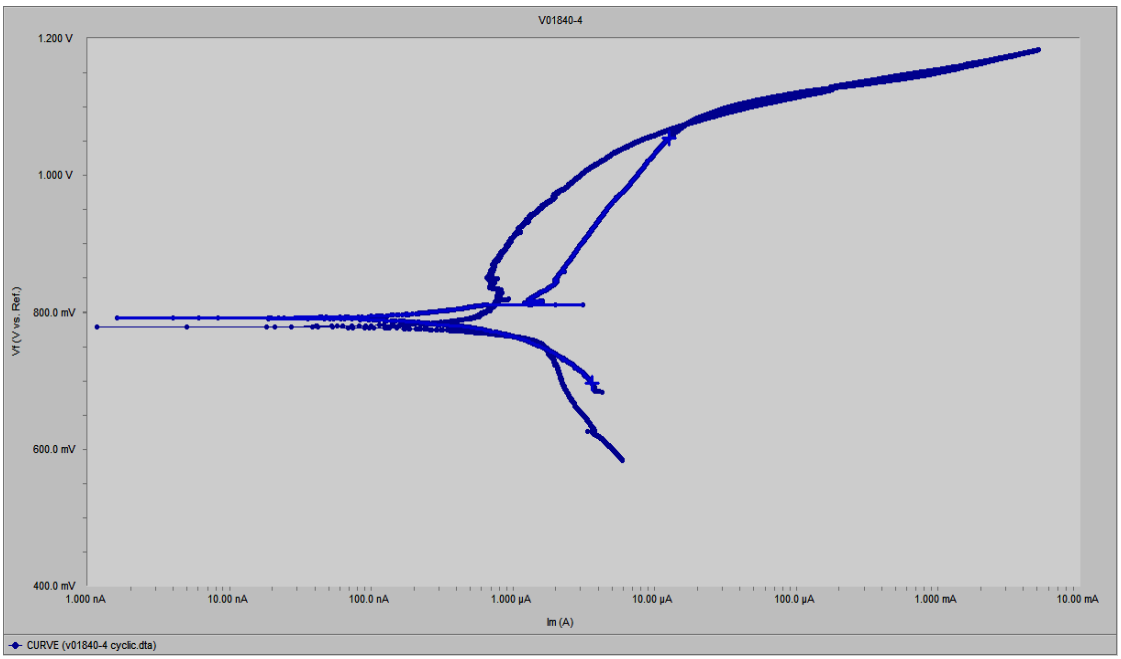

Fig.12 Polarization Curve of Hastelloy MO-10 weld cladding, Location.3

In Figure 10, 11, and 12, the vertical axis represents the corrosion potential, while the horizontal axis represents the current density. The corrosion potential (Ecorr), corrosion current densities (Icorr), and the anodic and cathodicTafel slopes (βa and βc) are listed in Table 8.

Table 8: Corrosion Potential Test Parameters

Parameter	Observation		
	Sample 1	Sample 2	Sample 3
Sample Size (cm)	1L X 1W	1L X 1W	1L X 1W
Test Solution	Ferric Sulphate + Sulphuric Acid	Ferric Sulphate + Sulphuric Acid	Ferric Sulphate + Sulphuric Acid
Beta A (V/decade)	363.9e-3	1.169	367.5e-3
Beta C (V/decade)	123.0e-3	58.50e-3	231.6e-3
Corrosion Current (Icorr)	2.210 (µA)	8.7 (µA)	2.050 (µA)
Corrosion Potential (Ecorr)(mV)	757.0	714.0	792.0
Corrosion Rate (mpy)	**1.129**	**4.435**	**1.045**

Comparing the results presented in Table 8 with the corrosion rate in mpy at various locations of the Hastelloy MO-10 Weld cladding, the average corrosion rate of the Hastelloy MO-10 weld cladding on SS 316L achieved through SMAW is 2.20 mpy.

Conclusions

This research study aimed to investigate the utilization of ENiCrMo-10, providing valuable insights into the performance and characteristics of the weld cladding, with implications for its potential applications in the petrochemical industry. The findings are as follows:

- The Hastelloy Mo-10 weld cladding exhibited a clean surface without welding flaws, indicating good weldability. Some issues were observed at the starting and ending points of the automated welding process, attributed to setup problems in operational parameters. Overall, the surface quality of the weld cladding was deemed adequate.
- The Shielded Metal Arc welding process achieved adequate penetration of the Hastelloy weld cladding into the base metal, resulting in a defect-free weld cladding confirmed by Macro and Visual examination.
- Bend test analysis confirmed that the welds were free from cracks or holes, demonstrating the reliability and optimal parameters of the welding procedure. The integration between the cladding layer and the AISI 316L SS substrate was found to be satisfactory.
- Hardness values were highest in the heat-affected zone (HAZ), followed by the weld cladding and base metal.
- Chemical composition analysis revealed that the weld cladding closely matched the targeted composition of ENiCrMo-10 once a depth of 3mm from the base metal was reached. Notably, at a depth of 2.5mm from the base metal, the composition of the weld cladding closely resembled ENiCrMo-10, exceptfor the Fe content in that specific area. The region between 2mm and 2.5mm depth is under scrutiny for further investigation. By exercising precise control over welding parameters, there is a promising opportunity to achieve the desired weld metal chemistry at a depth of 1mm, which holds significant potential for repair applications within various industries.
- Microstructure analysis revealed a defect-free weld cladding and an unchanged microstructure of the base metal. The SMAW process resulted in a heat-affected zone and a fine columnar interdendritic microstructure.
- Corrosion potential testing indicated that the average corrosion rate of the Hastelloy MO-10 weld cladding on SS 316L achieved through SMAW was 2.20 mpy.

Overall, these findings highlight the successful utilization of Hastelloy MO-10 for weld cladding on Grade 316L using the SMAW process. The research contributes to the understanding of the weldability, structural integrity, hardness characteristics, and corrosion resistance of this novel material combination. The results demonstrate the suitability of the weld cladding for

repair and cladding applications in the petrochemical industry, pharmaceutical industry, and oil and gas industry, offering numerous benefits such as precise control, sound welds, high-quality finish, cost reduction, and streamlined production efficiency. Further research and optimization of welding parameters can enhance the performance and broaden the potential applications of this material combination.

Acknowledgements:

The authors are thankful to GMM Pfaudler Ltd., Karamsad, Anand, Gujarat India, for providing machines and materials to perform necessary experimental work.

References:

[1] International Labour organization, *The Future of Work in the Oil and Gas Industry*, no. December. 2022.

[2] C. A. Mendes Da Mota, A. Saldanha do Nascimento, D. Neves Garcia, D. A. Silva da Silva, F. Ribeiro Teixeira, and V. A. Ferraresi, "Nickel overlay deposited by MIG welding and cold wire MIG welding," *Weld. Int.*, vol. 32, no. 9, pp. 588–598, 2018, doi: 10.1080/09507116.2017.1347333.

[3] T. Materials and I. Company, "Properties and Selection: Nonferrous Alloys and Special-Purpose Materials," Prop. Sel. Nonferrous Alloy. Spec. Mater., 1990, doi: 10.31399/asm.hb.v02.9781627081627.

[4] Mehta, M. V., Vora, J. J., & Chaudhari, M. D. (2021). A Review of Challenges to Hastelloy – C Series Weld Overlay. In *Recent Advances in Mechanical Infrastructure* (pp. 157–172). Lecture Notes in Intelligent Transportation and Infrastructure. https://doi.org/10.1007/978-981-33-4176-0_13

[5] A. Scheid and A. S. C. M. de Oliveira, "Analysis of PTA hardfacing with CoCrWC and CoCrMoSi alloys," Soldag. Inspeção, vol. 18, no. 4, pp. 322–328, 2013, doi: 10.1590/s0104-92242013000400004.

[6] E. R. Sharma, E. M. Kumar, and D. A. Kamboj, "Hastelloy C-276Weld Overlay bySMAW Process," Int. J. Eng. Res. Appl., vol. 07, no. 05, pp. 86–91, 2017, doi: 10.9790/9622-0705038691.

[7] A. Gatto, E. Bassoli, and M. Fornari, "Plasma Transferred Arc deposition of powdered high performances alloys: Process parameters optimisation as a function of alloy and geometrical configuration," Surf. Coatings Technol., vol. 187, no. 2–3, pp. 265–271, 2004, doi: 10.1016/j.surfcoat.2004.02.013.

[8] M. M. da Silva, V. R. Batista, T. M. Maciel, M. A. dos Santos, and T. L. Brasileiro, "Optimization of submerged arc welding process parameters for overlay welding," Weld. Int., vol. 32, no. 2, pp. 122–129, 2018, doi: 10.1080/09507116.2017.1347325.

[9] S. R. V Kumar, C Lee, G Verhaeghe, "CRA Weld Overlay - Influence of Welding Process and Parameters on Dilution and Corrosion Resistance," TWI limited, 2010. https://www.twi-global.com/technical-knowledge/published-papers/cra-weld-overlay-influence-of-welding-process-and-parameters-on-dilution-and-corrosion-resistance#:~:text=TIG and MIG welding processes,was generally less than 40%25.

[10] S. Analytics et al., "dissimilares com a superliga à base de níquel," 2019.

[11] D. D. Deshmukh and V. D. Kalyankar, "Deposition Characteristics of Multitrack Overlayby Plasma Transferred Arc Welding on SS316Lwith Co-Cr Based Alloy-Influence ofProcess Parameters," High Temp. Mater. Process., vol. 38, no. 2019, pp. 248–263, 2019, doi: 10.1515/htmp-2018-0046.

[12] A. Volpi and G. Serra, "Weld Overlay of Highly Corrosion Resistant Nickel Chromium," ASME 2018 Symp. Elev. Temp. Appl. Mater. Foss. Nucl. Petrochemical Ind., pp. 1–12, 2018.

[13] R. Ranjan and A. Kumar Das, "Protection from corrosion and wear by different weld cladding techniques: A review," Mater. Today Proc., vol. 57, pp. 1687–1693, 2022, doi: 10.1016/j.matpr.2021.12.329.

[14] B. Khara, N. D. Mandal, A. Sarkar, M. Sarkar, B. Chakrabarti, and S. Das, "Weld Cladding with Austenitic Stainless Steel for Imparting Corrosion Resistance," Indian Weld. J., vol. 49, no. 1, p. 74, 2016, doi: 10.22486/iwj.v49i1.125902.

[15] M. Sowrirajan, P. Koshy Mathews, and S. Vijayan, "Simultaneous multi-objective optimization of stainless steel clad layer on pressure vessels using genetic algorithm," J. Mech. Sci. Technol., vol. 32, no. 6, pp. 2559–2568, 2018, doi: 10.1007/s12206-018-0513-1.

[16] T. Kannan and J. Yoganandh, "Effect of process parameters on clad bead geometry and its shape relationships of stainless steel claddings deposited by GMAW," Int. J. Adv. Manuf. Technol., vol. 47, no. 9–12, pp. 1083–1095, 2010, doi: 10.1007/s00170-009-2226-1.

[17] N. M. and R.S. and Parmar, "Effects of welding process parameters on the geometry and dilution of the bead in the automatic surfacing," J. Mater. Process. Technol., vol. 41, pp. 244–247, 2010.

[18] P. K. Palani and N. Murugan, "Optimization of weld bead geometry for stainless steel claddings deposited by FCAW," J. Mater. Process. Technol., vol. 190, no. 1–3, pp. 291–299, 2007, doi: 10.1016/j.jmatprotec.2007.02.035.

[19] J. L. Caron and J. W. Sowards, Weldability of Nickel-Base Alloys, vol. 6, no. October. 2014. doi: 10.1016/B978-0-08-096532-1.00615-4.

[20] C. M. Lin, T. L. Su, and K. Y. Wu, "Effects of parameter optimization on microstructure and properties of GTAW clad welding on AISI 304L stainless steel using Inconel 52M," Int. J. Adv. Manuf. Technol., vol. 79, no. 9–12, pp. 2057–2066, 2015, doi: 10.1007/s00170-015-6875-y.

[21] Haynes International Inc., "Haynes International, Physical properties of C-22," Haynes International. https://www.haynesintl.com/alloys/alloy-portfolio_/Corrosion-resistant-Alloys/HASTELLOY-C-22/physical-properties (accessed Jun. 01, 2020).

[22] Haynes International, "Fabrication of Hastelloy ®," H-2010f, 2003. http://specialmetals.ir/images/technical_info/Total/hastelloys.pdf (accessed Jun. 01, 2020).

[23] Haynes International Inc., "HASTELLOY ® C-2000 ® alloy," H-2118A, 2017.

[24] A. S. M. International and A. Rights, ASM specialty handbook: nickel, cobalt, and their alloys, vol. 38, no. 11. 2001. doi: 10.5860/choice.38-6206.

[25] T. A. M. Haemers, D. G. Rickerby, F. Lanza, F. Geiger, and E. J. Mittemeijer, "Laser cladding of stainless steel with Hastelloy," Adv. Eng. Mater., vol. 3, no. 4, pp. 242–245, 2001, doi: 10.1002/1527-2648(200104)3:4<242::AID-ADEM242>3.0.CO;2-D.

[26] S. Zhou, G. Ma, W. Dongjiang, D. Chai, and M. Lei, "Ultrasonic vibration assisted laser welding of nickel-based alloy and Austenite stainless steel," J. Manuf. Process., vol. 31, pp. 759–767, 2018, doi: 10.1016/j.jmapro.2017.12.023.

[27] V. Advaith, A. Vaisikan, S. Thirumalini, R. Padmanaban, M. Arivarasu, and T. Ram Prabhu, "Comparative studies on pulsed GTAW and AGTAW on dissimilar alloy C-22 and AISI 316L weldments," Mater. Today Proc., vol. 27, no. xxxx, pp. 2886–2895, 2019, doi: 10.1016/j.matpr.2020.01.613.

[28] H.-2019A Hayens International, "HASTELLOY ® C-22 ® alloy," Hast. Int., vol. H-2019A, 2020, [Online]. Available: http://haynesintl.com/docs/default-source/pdfs/new-alloy-brochures/corrosion-resistant-alloys/brochures/c-22-brochure.pdf?sfvrsn=fd7929d4_22

[29] M. V. Mehta, J. J. Vora, and M. D. Chaudhari, "A Review of Challenges to Hastelloy – C Series Weld Overlay," 2021, pp. 157–172. doi: 10.1007/978-981-33-4176-0_13.

[30] N. Di, "Guidelines for the welded fabrication of nickel alloys for the welded fabrication of nickel alloys for corrosion-resistant service," Nickel Dev. Inst., no. Series No 11 012,1994, pp. 29–43, 1994.

[31] G. Requirements, R. Documents, and C. Composition, "Specification for Chromium and Chromium- Nickel Stainless Steel Plate , Sheet , and Strip for Pressure Vessels and for," 2007.

[32] A. O. Brien, Welding Handbook, vol. 1. 1969. doi: 10.1007/978-1-349-00324-2.

[33] B. H. Yoon, Y. S. Ahn, and C. H. Lee, "The effect of dilution on HAZ liquation cracking in PTAW Ni-base superalloys overlay deposit," ISIJ Int., vol. 42, no. 2, pp. 178–183, 2002, doi: 10.2355/isijinternational.42.178.

[34] S. Neyka, M. Kusch, and P. Mayr, "Progress in high performance hardfacing processes tandem-gas-metal-arc- welding and plasma-MIG hybrid welding," ASM Proc. Int. Conf. Trends Weld. Res., no. February 2018, pp. 784–790, 2013.

[35] Y. Guo, D. Wu, G. Ma, and D. Guo, "Trailing heat sink effects on residual stress and distortion of pulsed laser welded Hastelloy C-276 thin sheets," J. Mater. Process. Technol., vol. 214, no. 12, pp. 2891–2899, 2014, doi: 10.1016/j.jmatprotec.2014.06.012.

[36] J. Santander, L. Fonseca, S. Udina, and S. Marco, "Ac ce pte d M us p," 2007, doi: 10.1016/j.snb.2007.07.003.

[37] A. S. C. M. D'Oliveira, R. Vilar, and C. G. Feder, "High temperature behaviour of plasma transferred arc and laser Co-based alloy coatings," Appl. Surf. Sci., vol. 201, no. 1–4, pp. 154–160, 2002, doi: 10.1016/S0169-4332(02)00621-9.

[38] H. Deng, H. Shi, and S. Tsuruoka, "Influence of coating thickness and temperature on mechanical properties of steel deposited with Co-based alloy hardfacing coating," Surf. Coatings Technol., vol. 204, no. 23, pp. 3927–3934, 2010, doi: 10.1016/j.surfcoat.2010.05.013.

[39] V. Balasubramanian, R. Varahamoorthy, C. S. Ramachandran, and C. Muralidharan, "Selection of welding process for hardfacing on carbon steels based on quantitative and qualitative factors," Int. J. Adv. Manuf. Technol., vol. 40, no. 9–10, pp. 887–897, 2009, doi: 10.1007/s00170-008-1406-8.

[40] C. Sudha, P. Shankar, R. V. S. Rao, R. Thirumurugesan, M. Vijayalakshmi, and B. Raj, "Microchemical and microstructural studies in a PTA weld overlay of Ni-Cr-Si-B alloy on AISI 304L stainless steel," Surf. Coatings Technol., vol. 202, no. 10, pp. 2103–2112, 2008, doi: 10.1016/j.surfcoat.2007.08.063.

[41] S. Mandal, S. Kumar, P. Bhargava, C. H. Premsingh, C. P. Paul, and L. M. Kukreja, "An experimental investigation and analysis of PTAW process," Mater. Manuf. Process., vol. 30, no. 9, pp. 1131–1137, 2015, doi: 10.1080/10426914.2014.984227.

[42] V. Balasubramanian, A. K. Lakshminarayanan, R. Varahamoorthy, and S. Babu, "Application of Response Surface Methodolody to Prediction of Dilution in Plasma Transferred Arc Hardfacing of Stainless Steel on Carbon Steel," J. Iron Steel Res. Int., vol. 16, no. 1, pp. 44–53, 2009, doi: 10.1016/S1006-706X(09)60009-1.

[43] R. R. Bharath, R. Ramanathan, B. Sundararajan, and P. B. Srinivasan, "Optimization of process parameters for deposition of Stellite on X45CrSi93 steel by plasma transferred arc technique," Mater. Des., vol. 29, no. 9, pp. 1725–1731, 2008, doi: 10.1016/j.matdes.2008.03.020.

[44] S. Buytoz, A. Orhan, A. K. Gur, and U. Caligulu, "Microstructural Development of Fe-Cr-C and B4C Powder Alloy Coating on Stainless Steel by Plasma-Transferred Arc Weld Surfacing," Arab. J. Sci. Eng., vol. 38, no. 8, pp. 2197–2204, 2013, doi: 10.1007/s13369-013-0599-9.

[45] F. Fernandes, B. Lopes, A. Cavaleiro, A. Ramalho, and A. Loureiro, "Effect of arc current on microstructure and wear characteristics of a Ni-based coating deposited by PTA on gray cast iron," Surf. Coatings Technol., vol. 205, no. 16, pp. 4094–4106, 2011, doi: 10.1016/j.surfcoat.2011.03.008.

[46] B. C. Oberländer and E. Lugscheider, "Comparison of properties of coatings produced by laser cladding and conventional methods," Mater. Sci. Technol. (United Kingdom), vol. 8, no. 8, pp. 657–665, 1992, doi: 10.1179/mst.1992.8.8.657.

[47] Q. Y. Wang, Y. F. Zhang, S. L. Bai, and Z. De Liu, "Microstructures, mechanical properties and corrosion resistance of Hastelloy C22 coating produced by laser cladding," J. Alloys Compd., vol. 553, pp. 253–258, 2013, doi: 10.1016/j.jallcom.2012.10.193.

[48] Q. Y. Wang, S. L. Bai, and Z. De Liu, "Corrosion behavior of Hastelloy C22 coating produced by laser cladding in static and cavitation acid solution," Trans. Nonferrous Met. Soc. China (English Ed., vol. 24, no. 5, pp. 1610–1618, 2014, doi: 10.1016/S1003-6326(14)63232-5.

[49] P. J. E. Monson and W. M. Steen, "Comparison of laser hardfacing with conventional processes," Surf. Eng., vol. 6, no. 3, pp. 185–193, 1990, doi: 10.1179/sur.1990.6.3.185.

[50] P. Balu, P. Leggett, S. Hamid, and R. Kovacevic, "Multi-response optimization of laser-based powder deposition of multi-track single layer hastelloy C-276," Mater. Manuf. Process., vol. 28, no. 2, pp. 173–182, 2013, doi: 10.1080/10426914.2012.677908.

[51] E. Toyserkani, A. Khajepour, and S. Corbin, "Laser Cladding Laser Cladding," New York, vol. 11, no. 2, p. 221, 2017, [Online]. Available: https://www.taylorfrancis.com/books/9781420039177

[52] Q. Y. Wang, S. L. Bai, and Z. De Liu, "Corrosion behavior of Hastelloy C22 coating produced by laser cladding in static and cavitation acid solution," Trans. Nonferrous Met. Soc. China (English Ed., vol. 24, no. 5, pp. 1610–1618, 2014, doi: 10.1016/S1003-6326(14)63232-5.

[53] C. P. Alvarães, F. C. A. Madalena, L. F. G. De Souza, J. C. F. Jorge, L. S. Araújo, and M. C. Mendes, "Performance of the INCONEL 625 alloy weld overlay obtained by FCAW process," Rev. Mater., vol. 24, no. 1, 2019, doi: 10.1590/s1517-707620190001.0627.

[54] A. Tahaei, F. G. Vazquez, M. Merlin, A. Arizmendi-Morquecho, F. A. R. Valdes, and G. L. Garagnani, "Metallurgical Characterization of a Weld Bead Coating Applied by the PTA Process on the D2 Tool Steel," Soldag. Inspeção, vol. 21, no. 2, pp. 209–219, 2016, doi: 10.1590/0104-9224/si2102.10.

[55] T. J. Antoszczyszyn, R. M. G. Paes, A. S. C. M. de Oliveira, and A. Scheid, "Impact of dilution on the microstructure and properties of Ni-based 625 alloy coatings," Soldag. Inspeção, vol. 19, no. 2, pp. 134–144, Jun. 2014, doi: 10.1590/0104-9224/SI1902.05.

[56] E. M. Miná, Y. C. da Silva, J. Dille, and C. Carvalho Silva, "Effect of dilution on the microstructure of AWS ERNiCrMo-14 alloy in overlay welding by the TIG process with cold wire feed," Weld. Int., vol. 32, no. 2, pp. 130–138, 2018, doi: 10.1080/09507116.2017.1347326.

[57] S.L.Correia, "21o CBECIMAT - Congresso Brasileiro de Engenharia e Ciência dos Materiais 09 a 13 de Novembro de 2014, Cuiabá, MT, Brasil," Investig. Mech. Prop. Magnes. Met. matrix Compos. with a fine Dispers. CeO2 Part., vol. 5738, no. 1, pp. 2665–2672, 2014, doi: 10.2466/pr0.1981.48.1.335.

[58] M. Ahmad, J. I. Akhter, M. Akhtar, M. Iqbal, E. Ahmed, and M. A. Choudhry, "Microstructure and hardness studies of the electron beam welded zone of Hastelloy C-276," J. Alloys Compd., vol. 390, no. 1–2, pp. 88–93, 2005, doi: 10.1016/j.jallcom.2004.08.031.

[59] G. Xu, M. Kutsuna, Z. Liu, and H. Zhang, "Characteristics of Ni-based coating layer formed by laser and plasma cladding processes," Mater. Sci. Eng. A, vol. 417, no. 1–2, pp. 63–72, 2006, doi: 10.1016/j.msea.2005.08.192.

[60] T. J. Antoszczyszyn, R. M. G. Paes, A. S. C. M. de Oliveira, and A. Scheid, "Impact of dilution on the microstructure and properties of Ni-based 625 alloy coatings," Soldag. Inspeção, vol. 19, no. 2, pp. 134–144, 2014, doi: 10.1590/0104-9224/si1902.05.

[61] P. Varghese, E. Vetrivendan, M. K. Dash, S. Ningshen, M. Kamaraj, and U. Kamachi Mudali, "Weld overlay coating of Inconel 617 M on type 316 L stainless steel by cold metal transfer process," Surf. Coatings Technol., vol. 357, pp. 1004–1013, 2019, doi: 10.1016/j.surfcoat.2018.10.073.

[62] A. E. Yaedu, A. S. C. M. D. Oliveira, A. E. Yaedu, and A. S. C. M. D. Oliveira, "Cobalt based alloy PTA hardfacing on different substrate steels Cobalt based alloy PTA hardfacing on different substrate steels," vol. 0836, no. March, 2016, doi: 10.1179/174328413X13789824293380.

[63] É. M. Miná, Y. C. da Silva, J. Dille, and C. C. Silva, "The Effect of Dilution on Microsegregation in AWS ER NiCrMo-14 Alloy Welding Claddings," Metall. Mater. Trans. A Phys. Metall. Mater. Sci., vol. 47, no. 12, pp. 6138–6147, 2016, doi: 10.1007/s11661-016-3786-y.

[64] Shravan C, Radhika N, Deepak Kumar N. H., & Sivasailam B. (2023). A review on welding techniques: properties, characterisations and engineering applications. Review Article. Published online: March 5, 2023. https://doi.org/10.1080/2374068X.2023.2186638

[65] Joshi, A., Parkash, S., & Kumar, M. (2018). Study of Mechanical Properties, Microstructure and Corrosion Behavior of Super Duplex-2594 Weld Overlay on Carbon Steel Substrate by Smaw. Journal of Engineering Research and Application, 8(7 Part-I), 65-70. ISSN: 2248-9622. DOI: 10.9790/9622-0807016570

[66] Kumar, V., Chandrasekhar, N., Albert, S. K., & Jayapandian, J. (2016). Analysis of arc welding process using Digital Storage Oscilloscope. Measurement, 81, 1-12. https://doi.org/10.1016/j.measurement.2015.11.031

[67] Sim, B.-M., Tang, S.-H., Alrifaey, M., & Jong, E.-N. T. (2022). Analyzing the Effects of Heat Treatment on SMAW Duplex Stainless Steel Weld Overlays. Materials, 15(5), 1833. https://doi.org/10.3390/ma15051833